An Investigation of Stepped Open Slot Antenna with Circular Tuning Stub

Prashant Purohit*, Bhupendra K. Shukla, and Deepak K. Raghuvanshi

Abstract—In this article, a microstrip-fed stepped open slot antenna is presented which is suitable for GSM 1800, WiFi, WiMAX, PCS, and ITM-2000 applications. The proposed geometry is composed of a circle-shaped tuning stub, a feed structure, and deformed ground plane. The proper tuning of resonating modes (f_{r1}, f_{r2}, f_{r3} and f_{r4}) and wideband frequency response are acquired by adjusting the dimension of stairs, tuning the stub and an elliptical slot. The experimental result demonstrates that this antenna covers the frequency range from 1.375 to 5.6 GHz with measured fractional bandwidth ($BW(\%) = 200 * (f_h - f_l)/(f_h + f_l)$) of 121.14% for $S_{11} < -10$ dB. This antenna also exhibits resonance at frequencies (measured) 1.625, 2.52, 2.82, 3.75, 4.67, and 5.42 GHz. After investigating the surface current distribution, the mathematical equations are deduced for simulated resonating frequencies of 1.35, 2, 3.8, and 5.22 GHz. Due to asymmetry in structure, asymmetric far-field patterns are found in E-plane with omnidirectional patterns in H-plane.

1. INTRODUCTION

The broadband feature of a planar antenna depends on the overlapping of resonating modes which can be achieved by choosing a proper dimension of the tuning stub and other elements of the antenna [1]. Many reported configurations, such as wide slot antenna [2–4], monopole antenna [5], and CPW fed monopole [6], are famous in the wireless industry due to their attractive features, such as wide impedance bandwidth, low profile, low cost, and easy integration with microwave circuitry. Due to half wavelength resonance, the size of above-mentioned antennas is large which is their main demerit. In the present scenario, the requirement of a compact antenna with wide impedance bandwidth is increasing. Printed open slot antenna is a potential candidate which offers compactness due to quarter wavelength resonance [7]. In addition, open slot antenna exhibits the ability to produce circular polarization and asymmetric radiation pattern due to its asymmetric geometry [8, 9]. The role of slots is prominent in above-mentioned antennas. Indeed, slots modify the path length of surface current vector which changes the position of resonating frequency. It also alters the effective capacitance and inductance of the antenna which directly affects the phase velocity ($v_p = 1/\sqrt{LC}$) of the resonating frequency [10–12]. Loading of the slot on the ground plane and patch provides new edges for fringing and also produces new resonating frequencies [13]. The impedance bandwidth of the open slot antenna can be modified by the following methods 1) By introducing notches on the circumference of the open slot which changes the resonant path length [7], 2) By cutting the steps on the open slot [14] which changes the mutual coupling between ground plane and radiating element, 3) By tapering the slot [15, 16]. The rotation of the radiating patch produces a large number of resonating modes, and by choosing the proper angle, these modes can be overlapped [17]. Some other methods are reported for enhancing the bandwidth of open slot antenna, such as integrating tuning stub [18], changing the shape of feed structure, and radiating element [19, 20].

In this communication, we design a stepped open slot antenna with a circular tuning element which is suitable for applications like GSM 1800, WiMAX, PCS and ITM-2000. The wide frequency response of this antenna is achieved by adjusting the dimension of the tuning stub, stair, and elliptical slot. It occupies the fractional bandwidth of 121.14% for $S_{11} < -10\,\mathrm{dB}$ that covers the frequency span from 1.375 to 5.6 GHz. The circuit model of the proposed antenna is also presented. At frequencies 1.35 GHz, 2 GHz, 3.8 GHz, and 5.22 GHz, the surface current distribution is analyzed, and the mathematical equations are deduced.

2. ANTENNA CONFIGURATION

The physical structure and parameters of the proposed antenna are depicted in Figure 1. It contains slot loaded ground plane, a feed structure, and a circular tuning stub. This antenna is placed on $XY = 0$ plane and fabricated on an FR-4 substrate with the dimension of 66 mm × 45 mm. The properties of the chosen substrate are tangent loss $\tan(\delta) = 0.02$, permittivity $\varepsilon_r = 4.3$, and height $h = 1.6$ mm. The thickness of the conducting layer is taken 0.035 mm. The circular tuning stub with radius R_t and feed structure $(F_w \times F_l)$ are designed on the top face of the substrate. In numerical analysis, this structure is excited by waveguide port. In the ground plane, an elliptical slot with parameters R_y (semi minor axis radius) and R_x (semi major axis radius) is etched which improves the impedance matching of the antenna in the interested frequency band. Further, stairs of uneven size are introduced which changes the location of resonating frequencies and impedance bandwidth of the antenna. The parameters of the stairs are S_{l1}, S_{w1} (first step), S_{l2}, S_{w2} (second step), and S_{l3}, S_{w3} (third step). To enhance the impedance bandwidth of the antenna, a rectangular shaped slot with size 23 mm × 20 mm is truncated on the left bottom side of the ground plane. Table 1 shows the dimension of the proposed antenna.
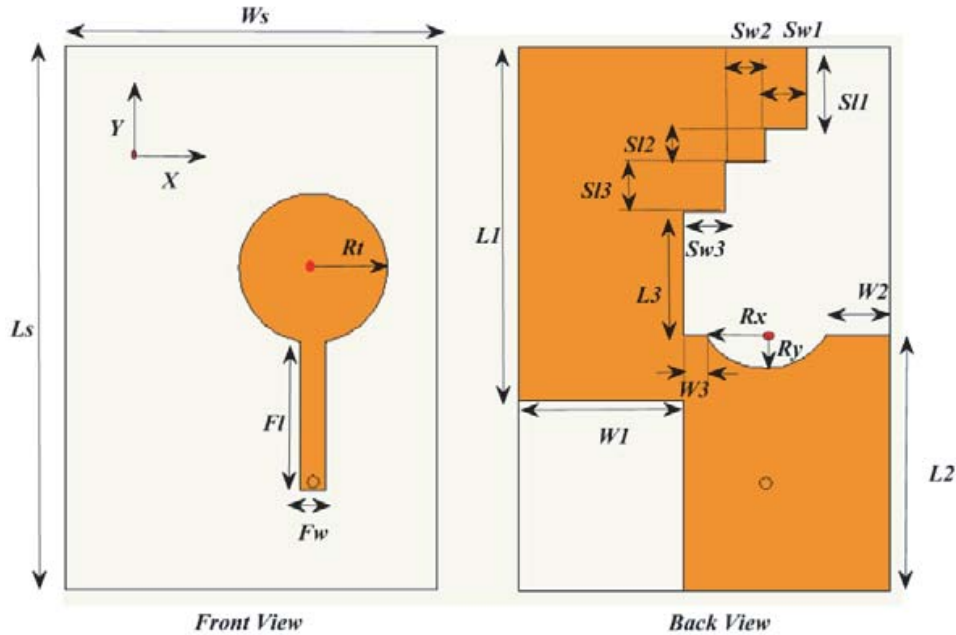
Figure 1. Configuration of the propose stepped open slot antenna with circular tuning element.

3. EVOLUTION OF PROPOSED STEPPED OPEN SLOT ANTENNA

The development of the proposed stepped open slot antenna is displayed in Figure 2. It is noticed that the shape of the ground plane is customized in succeeding stages. Figure 3 displays the comparison of reflection coefficient characteristics of the antennas, and performances of all antennas are listed in Table 2. Antenna 1 comprises an inverted L-shaped slot in the ground plane and a circular tuning stub. It shows dual-band characteristic with two resonating frequencies (see Table 2). By loading the slot, the

Table 1. The dimension of the stepped open slot antenna with circular tuning element.

Parameter	Dimension (mm)	Parameter	Dimension (mm)	Parameter	Dimension (mm)	Parameter	Dimension (mm)
F_w	3	W_s	45	R_y	7	S_{l2}	4
F_l	19	L_1	43	W_2	7.77	S_{w2}	5
R_t	9	L_2	31	W_3	2.77	S_{l3}	6
R_x	8	L_3	15	S_{l1}	10	S_{w3}	5
L_s	66	W_1	20	S_{w1}	5		

Table 2. Performance of antenna 1, 2, 3, 4 and 5.

Name of Antenna	Response	Band	Bandwidth (%)	Resonance frequency (GHz)
A1	Dual	1.67 to 1.87 GHz	11.29	1.77, 5.42
		5.00 to 6.00 GHz	18.18	
A2	Dual	1.65 to 1.92 GHz	15.12	1.77, 3.475
		2.77 to 4.45 GHz	46.53	
A3	Dual	1.35 to 2.25 GHz	50	1.75, 4.125
		2.62 to 4.42 GHz	51.13	
A4	Single	1.35 to 5.60 GHz	122.30	1.47, 1.95, 3.87, 5.2
A5	Single	1.27 to 5.62 GHz	126.27	1.35, 2, 3.8, 5.22
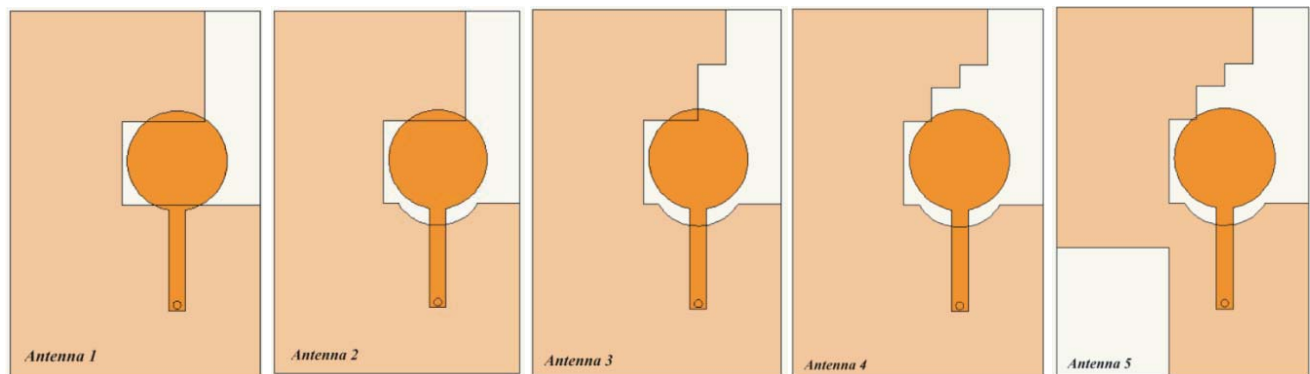
Figure 2. Schematic of evolution of the stepped open slot antenna with circular element.

effective inductance and capacitance of the antenna can be changed which modifies the bandwidth and position of resonating frequencies [8]. In the next step (antenna 2), an elliptical slot is introduced on the circumference of the inverted L-shaped slot. Due to this modification, impedance matching is raised in lower and mid frequency bands while resonance frequency at 5.42 GHz has disappeared. Further, the stair (antenna 3) is created on the ground plane that upgrades the coupling between slot and tuning stub. To achieve wideband response and upgrade the capacitive coupling between the slot and tuning stub, another step of the stair (antenna 4) is introduced which refines the impedance matching throughout the frequency band. Antenna 4 shows the impedance bandwidth of 122.30% from 1.35 to 5.6 GHz for $S_{11} < -10$ dB with four resonating frequencies. To modify the position of lower and higher cutoff frequencies, a rectangle-shaped slot is truncated on the left bottom side of the ground plane. Antenna 5 covers a frequency band from 1.27 to 5.62 GHz and exhibits the bandwidth of 126.27% for $S_{11} < -10$ dB.
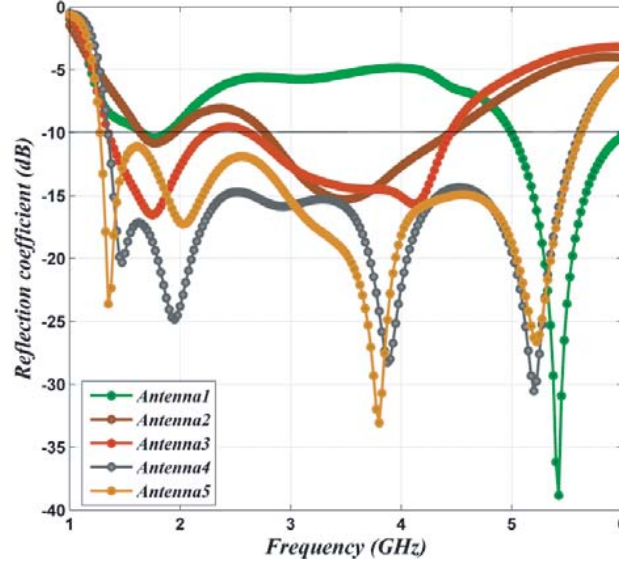
Figure 3. Comparison of reflection coefficient characteristics of antenna 1, 2, 3, 4, and 5.

4. CIRCUIT MODEL OF PROPOSED STEPPED OPEN SLOT ANTENNA

The circuit model of probe-fed patch antenna is shown in Figure 4. It is the parallel combination of inductance (L_1), capacitance (C_1), and resistance (R_1) [21–23].
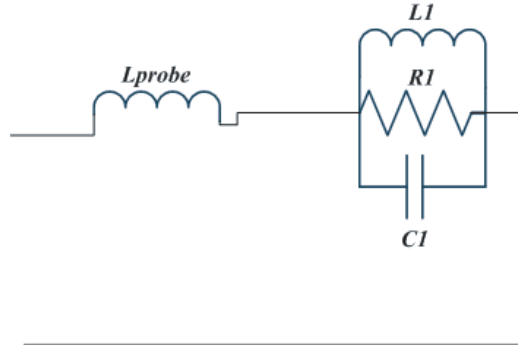
Figure 4. Circuit model of the rectangular patch antenna.

The values of L_1, C_1, and R_1 can be calculated by the following equations [21–23].

$$C_1 = \frac{LW\varepsilon_0\varepsilon_e}{2h}\cos^2\left(\frac{\pi x_0}{L}\right) \tag{1}$$

$$R_1 = \frac{Q}{\omega_r^2 C_1} \tag{2}$$

$$L_1 = \frac{1}{C_1\omega_r^2} \tag{3}$$

$$Q = \frac{c\sqrt{\varepsilon_e}}{4fh} \tag{4}$$

where L and W are the length and width of the patch. x_0 and ε_e are the feed location and effective permittivity of the substrate. Q and h are the quality factor and height of the substrate, respectively.

The input impedance of the rectangular patch antenna is given by

$$Z_{in} = j\omega L_{probe} + 1 \Big/ \left(\frac{1}{R_1} + \frac{1}{j\omega L_1} + j\omega C_1 \right) \tag{5}$$

The equivalent circuit of the proposed antenna is depicted in Figure 5 which is the series connection of the parallel RLC circuit. The broad frequency response of this circuit model is acquired after the overlapping of a large number of the resonating modes. The position of resonating frequency depends on the values of L_i, C_i, and R_i, where i varies from 1 to 10. This circuit is modeled in two steps. In the first step, the values of R, L, and C are obtained from simulated reflection coefficient characteristic (using CST) at resonating frequencies. In the second step, the circuit is implemented in ADS, and these values are tuned to achieve a proper response. The total impedance of the proposed circuit model can be computed by equation below.

$$Z_{in} = \sum_{i=1}^{10} 1 \Big/ \left(\frac{1}{R_i} + \frac{1}{j\omega L_i} + j\omega C_i \right) \tag{6}$$
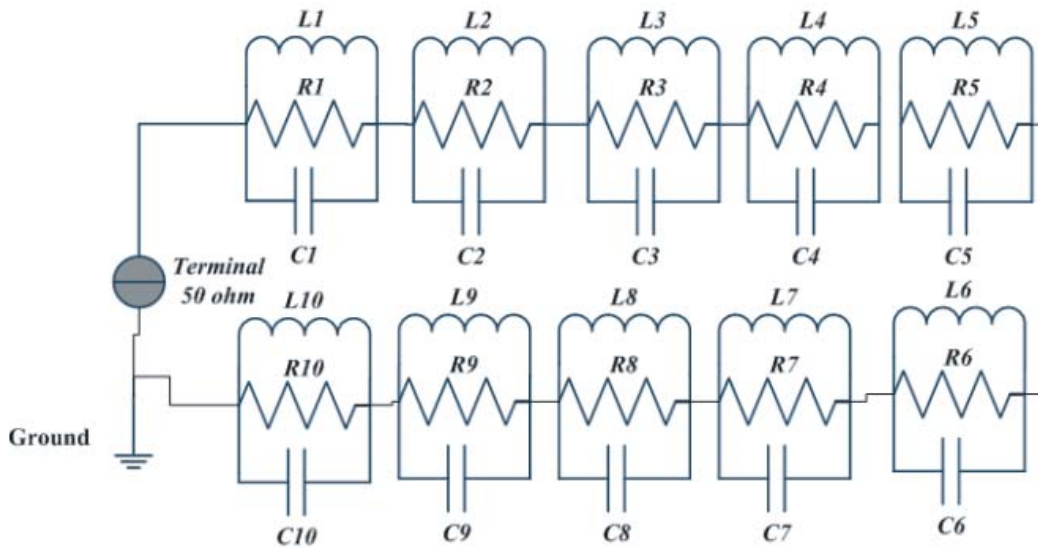
Figure 5. Circuit model of proposed stepped open slot antenna with circular tuning stub.

Table 3 represents the obtained values of R, L, and C from ADS. The comparison of reflection coefficient characteristics is shown in Figure 6. The red curve is the frequency response of the proposed circuit model.

5. TUNING OF PARAMETERS

5.1. Influence of Radius (R_t) of Circular Tuning Stub

The simulated reflection coefficient characteristic vs frequency for different values of R_t is depicted in Figure 7. By increasing R_t, the overlapping area increases with an open slot which affects the capacitive coupling between the slot and tuning stub. It is observed that this parameter critically affects the impedance bandwidth of the antenna. By increasing R_t up to 9 mm, the impedance matching in the lower and mid frequency bands is improved. For $R_t > 9$ mm, the bandwidth of the antenna is decreased due to over capacitive coupling.

5.2. Impact of Parameter of Stair (S_{l3} and S_{w3})

The effect of parameters of stair on reflection coefficient characteristic is displayed in Figure 8. The length of the stair (S_{l3}) mainly affects the impedance matching in the lower frequency band. With
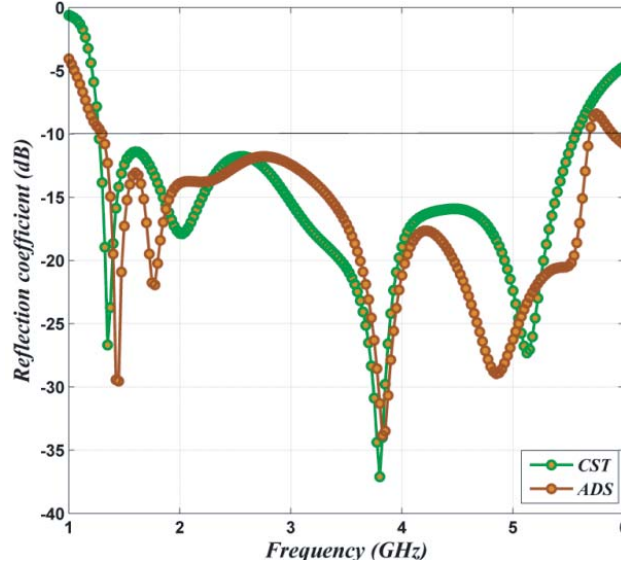
Figure 6. Comparison of frequency response obtained from CST and circuit simulation.

Table 3. Obtained value of R, L, C through CST and ADS.

Obtained Values from ADS					
Resistance (Ω)		Capacitance (pF)		Inductance (nH)	
R_1	25.115	C_1	27.36	L_1	0.32
R_2	44.083	C_2	9.422	L_2	1.924
R_3	40.68	C_3	25.02	L_3	0.555
R_4	28.008	C_4	11.455	L_4	0.1384
R_5	26.935	C_5	5.4	L_5	0.99
R_6	47.421	C_6	26.811	L_6	0.029
R_7	63.276	C_7	3.289	L_7	0.87
R_8	41.93	C_8	2.25	L_8	0.4016
R_9	54.155	C_9	4.284	L_9	0.1056
R_{10}	31.98	C_{10}	0.414	L_{10}	0.4895
Obtained Values from CST					
Resistance (Ω)		Capacitance (pF)		Inductance (nH)	
R_1	50.23	C_1	34.20	L_1	0.40
R_2	33.91	C_2	6.73	L_2	1.48
R_3	67.80	C_3	16.68	L_3	0.37
R_4	31.12	C_4	22.91	L_4	0.173
R_5	53.87	C_5	3.60	L_5	0.66
R_6	52.69	C_6	29.79	L_6	0.058
R_7	52.73	C_7	2.53	L_7	0.58
R_8	59.90	C_8	2.26	L_8	0.502
R_9	54.155	C_9	7.14	L_9	0.132
R_{10}	53.30	C_{10}	0.828	L_{10}	0.979
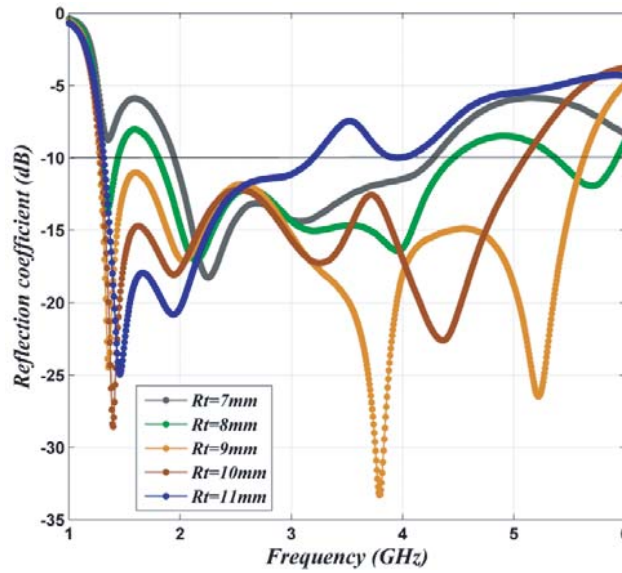
Figure 7. Simulated S_{11} versus frequency for different values of R_t of the proposed antenna.
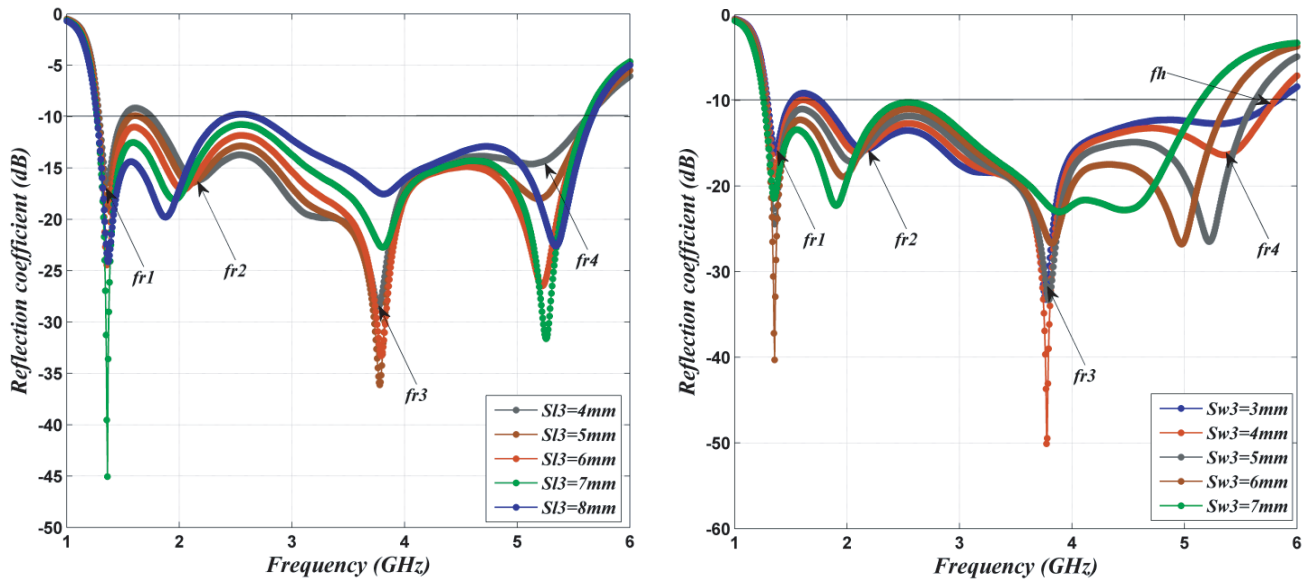
Figure 8. Simulated S_{11} versus frequency for different lengths and widths of stair.

increasing S_{l3}, the location of the second resonating frequency (f_{r2}) is shifted towards lower frequency band while frequencies f_{r1} and f_{r3} do not change their position. The width of the stair (S_{w3}) changes the position of the higher cutoff frequency (f_h) and bandwidth of the antenna. With increasing S_{w3}, the location of f_h is shifted towards lower frequency band. Due to this, the bandwidth of the antenna is reduced. The frequencies f_{r2} and f_{r4} are shifted towards lower frequency band. It is observed that the uneven impedance matching is found at f_{r1} and f_{r3}.

5.3. Influence of Radius (R_x and R_y) of the Elliptical Slot

The effect of R_x (major axis radius) and R_y (minor axis radius) on reflection coefficient characteristic of the proposed antenna is depicted in Figure 9. These two parameters affect the overlapping area of
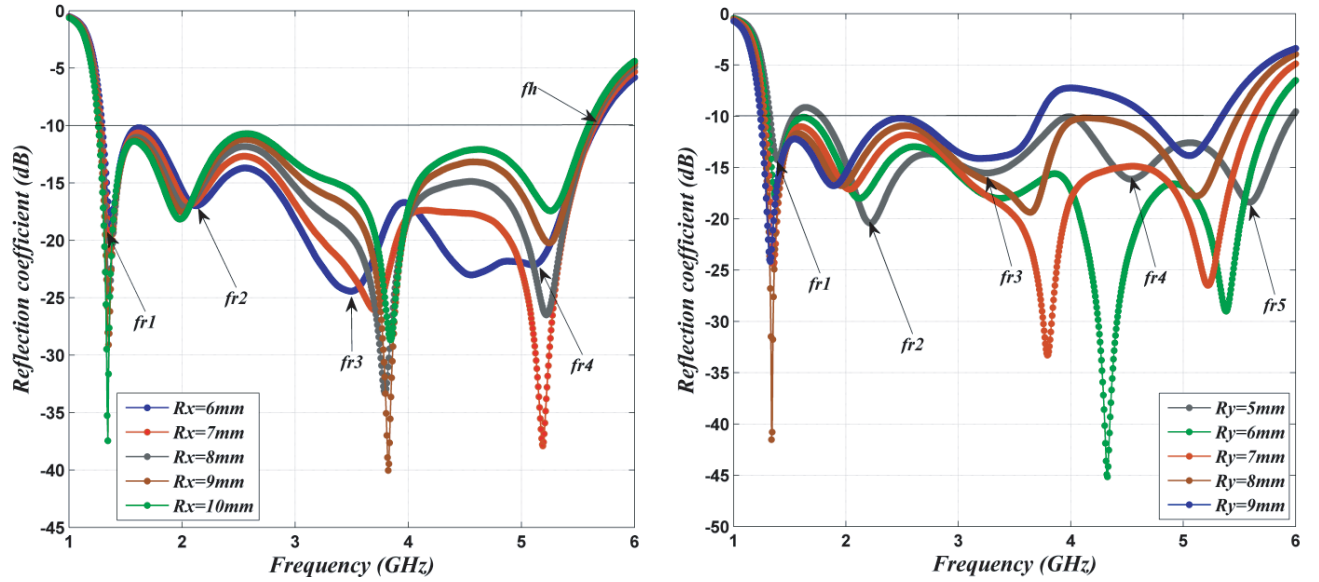
Figure 9. Simulated S_{11} versus frequency for different radii of elliptical slot.

open slot with tuning stub. It can be noticed that by the major axis radius only affects the impedance matching at frequencies f_{r1}, f_{r2}, f_{r3}, and f_{r4}. The resonance frequency f_{r2} is drifted toward lower frequency band with increasing the length of the major axis radius. The minor axis radius R_y critically affects the position of higher cutoff frequency and bandwidth of the antenna. With increasing R_y, the impedance matching is improved at lower frequency band while the resonating frequencies f_{r4} and f_{r5} are shifted in leftward direction.

6. EXPERIMENTAL RESULTS AND DISCUSSION

6.1. Reflection Coefficient Characteristic

The fabricated stepped open slot antenna with a circular tuning stub is shown in Figure 10. The simulated results and optimization of the antenna are achieved by CST Microwave Studio. The compared reflection coefficient characteristics of proposed antenna are shown in Figure 11. The measured results of input impedance and reflection coefficient are acquired from Agilent Technologies based Vector Network Analyzer N2223A in frequency range 1 to 6 GHz. The proposed antenna exhibits the measured fractional bandwidth of 121.14% for $S_{11} < -10$ dB which covers the frequency range from 1.375 to 5.6 GHz. This antenna also exhibits the resonance at frequencies (measured) 1.625, 2.52, 2.82, 3.75, 4.67, and 5.42 GHz. The simulated resonance is found at frequencies 1.375, 2, 3.8, and 5.22 GHz.

A small error of 7.2% between simulated and measured lower cutoff frequencies is estimated. It is noticed that the positions of measured and simulated resonating frequencies are not matched due to following reasons. 1) Connector and conductor loss, 2) Variation of dielectric constant. An error of 0.89% is also computed between measured and simulated higher cutoff frequencies. It is analyzed that the lower cutoff frequency (f_{lc}) of the proposed antenna is controlled by the dimension of the ground plane. The frequency formulation of f_{lc} is given below [11, 12].

$$P_1 = L_1 + W_1 + (L_s - L_1) + (W_s - W_1) \tag{7}$$

$$P_1 = L_s + W_s \tag{8}$$

$$f_{lc} = \frac{c}{P_1\sqrt{\varepsilon_r}} \tag{9}$$

where P_1 is the path length, and c and ε_r are the speed of light and permittivity of the substrate respectively. The calculated value of path length P_1 is 111 mm. By using Equation (9), the computed

Figure 10. Configuration of fabricate stepped open slot antenna with circular tuning element.
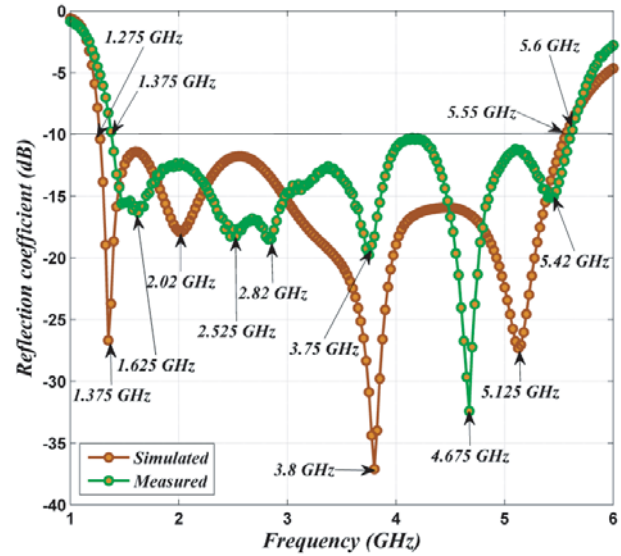
Figure 11. The compared reflection coefficient characteristic versus frequency plot.

value of f_{lc} is 1.29 GHz which is nearly equal to measured and simulated lower cutoff frequencies. An error of 1.16% is found between simulated and calculated f_{lc}.

6.2. Input Impedance

The compared input impedance of the proposed stepped open slot antenna is depicted in Figure 12. It is noticed that multiple loops are found inside of the VSWR circle. These loops indicate the mutual coupling and overlapping between resonating modes which are required for realization of wide impedance bandwidth.
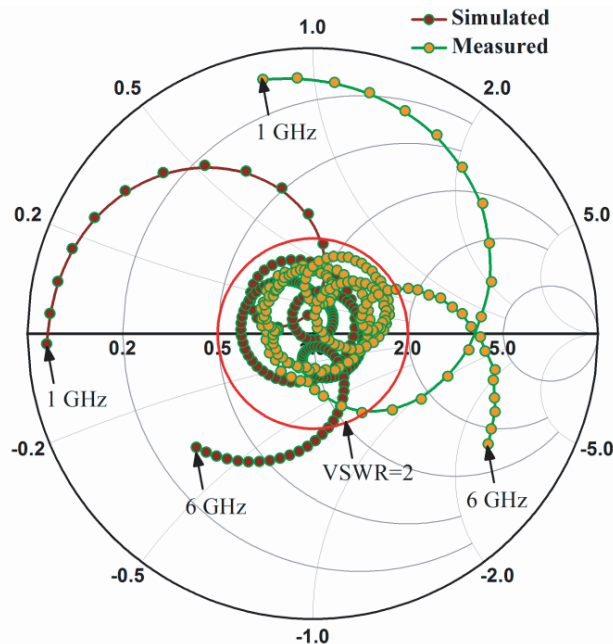
Figure 12. Compared input impedance characteristic of the proposed stepped open slot antenna.

6.3. Current Distribution

At simulated resonating frequencies, the surface current distribution of proposed antenna is investigated which is depicted in Figure 13. After excitation, the current vectors are scattered on tuning stub and slot loaded ground plane. At frequency 1.35 GHz, the current vectors sink towards right bottom corner of the ground plane, and maximum intensity of current is investigated near elliptical slot. This resonating frequency is developed due to stepped open slot and side edge of the ground plane. The frequency formulation of the first resonating frequency is given below [11, 12].

$$P_2 = S_{l1} + S_{w1} + S_{l2} + S_{w2} + S_{l3} + S_{w3} + L_3 + W_3 + L_2 + W_2 + E \tag{10}$$

$$E = 0.7 * \pi * \sqrt{(R_x^2 + R_y^2)/2} \tag{11}$$

$$f_1 = \frac{c}{P_2\sqrt{\varepsilon_r}} \tag{12}$$

where P_2 is the path length, and ε_r is the dielectric constant. The estimated value of P_2 is 108.02 mm. By using Equation (12), the calculated value of f_1 is 1.328 GHz. An error of 3.41% is estimated between the first simulated and calculated resonating frequencies. At frequency 2 GHz, the current vectors sink towards right top corner of the ground plane, and circulation of current vectors is also investigated on the tuning stub. This frequency is developed due to stepped open slot, and frequency formulation of
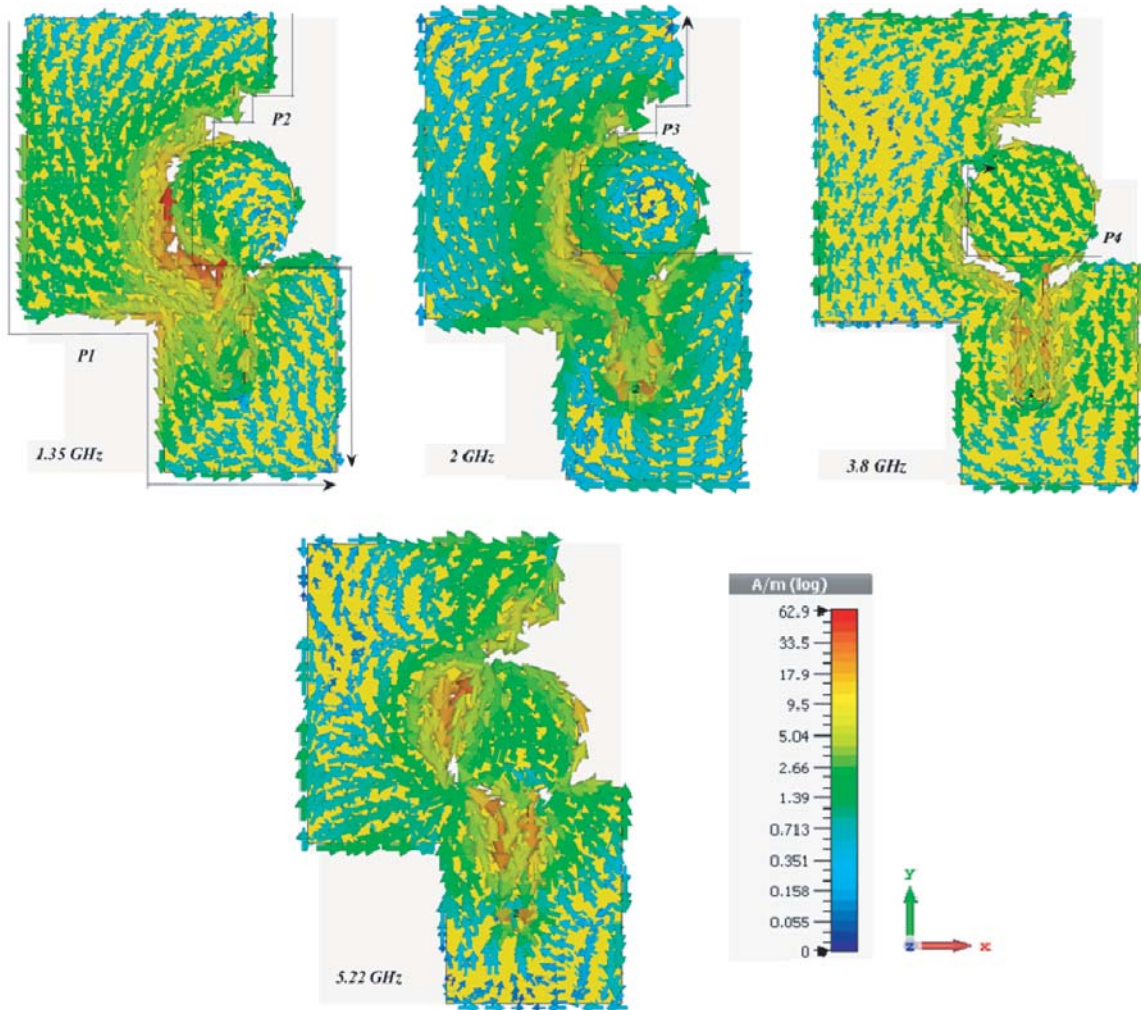
Figure 13. The simulated surface current distribution at frequency 1.35, 2, 3.8, and 5.22 GHz.

this second resonating frequency (f_2) is given below.

$$P_3 = S_{l1} + S_{w1} + S_{l2} + S_{w2} + S_{l3} + S_{w3} + L_3 + W_3 + W_2 + E \tag{13}$$

$$f_2 = \frac{c}{P_3\sqrt{\varepsilon_r}} \tag{14}$$

where P_3 is the path length, and the calculated value of P_3 is 77.02 mm. By using Equation (14), the calculated value of f_2 is 1.87 GHz which is nearly equal to 2 GHz. An error of 6.5% is found between simulated and computed second resonating frequencies. The resonance frequency 3.8 GHz (f_3) is generated due to open slot, and this frequency is estimated by following equations.

$$P_4 = L_3 + W_3 + (W_2/2) + E + (S_{w3}/2) \tag{15}$$

$$f_3 = \frac{c}{P_4\sqrt{\varepsilon_r}} \tag{16}$$

where P_4 is the path length, and the calculated value of P_4 is 40.675 mm. The calculated value of f_3 is 3.52 GHz. An error of 7.36% is found between simulated and computed third resonating frequencies. The fourth resonating frequency 5.22 GHz is developed due to the circular tuning element, and it is noticed that the current vectors are distributed like TM10 mode on this element.

$$P_5 = \pi * R_t \tag{17}$$

$$f_4 = \frac{c}{P_5\sqrt{\varepsilon_r}} \tag{18}$$

where P_5 is the half perimeter of circular tuning element, and the calculated value of P_5 is 28.26 mm. The calculated value of f_4 is 5.1 GHz which is nearly equal to 5.22 GHz.

6.4. Far Field Pattern

The comparison between simulated and measured radiation patterns at frequencies 1.35, 2, 3.8, and 5.22 GHz is displayed in Figure 14. We have noticed the asymmetric radiation (in E plane) pattern which is found due to asymmetry structure. At frequency 1.35 GHz, the pattern is omnidirectional in H plane while asymmetric pattern is found in E plane. The shape of the pattern is changed due to existence of higher order mode with fundamental mode. At frequencies 2, 3.8, and 5.22 GHz, the shape of the omnidirectional pattern is changed. The simulated patterns in E plane are almost similar in all resonating frequencies. Measured patterns slightly differ from the simulated ones because of multiple reasons: 1) radiation from the coaxial cable at lower frequency, 2) environment surrounding the measuring instruments, 3) measurement and fabrication error. Figure 15 exhibits the graph of simulated gain and efficiency versus frequency. The realized gain varies between 2.1 and 4.1 dBi. It is

(a)

(b)

(c)

(d)
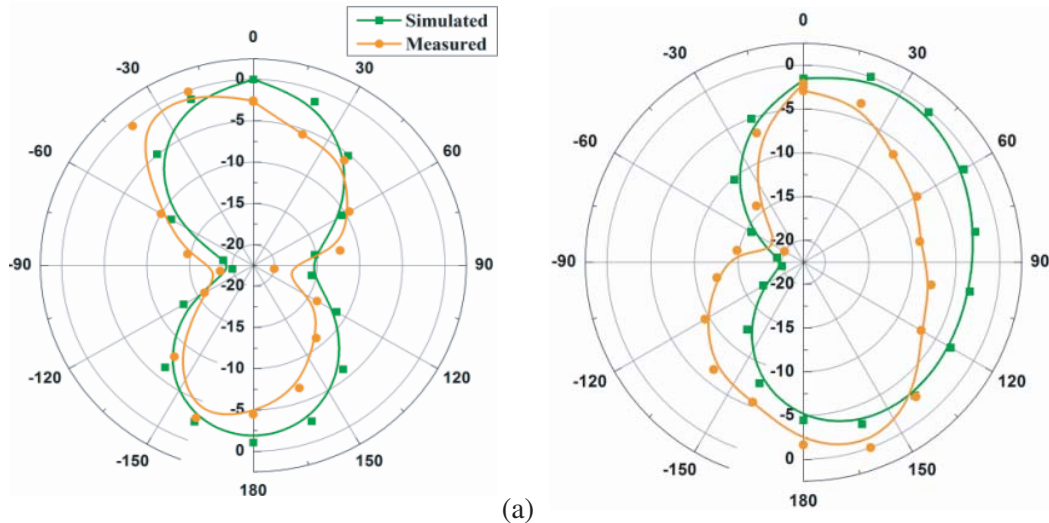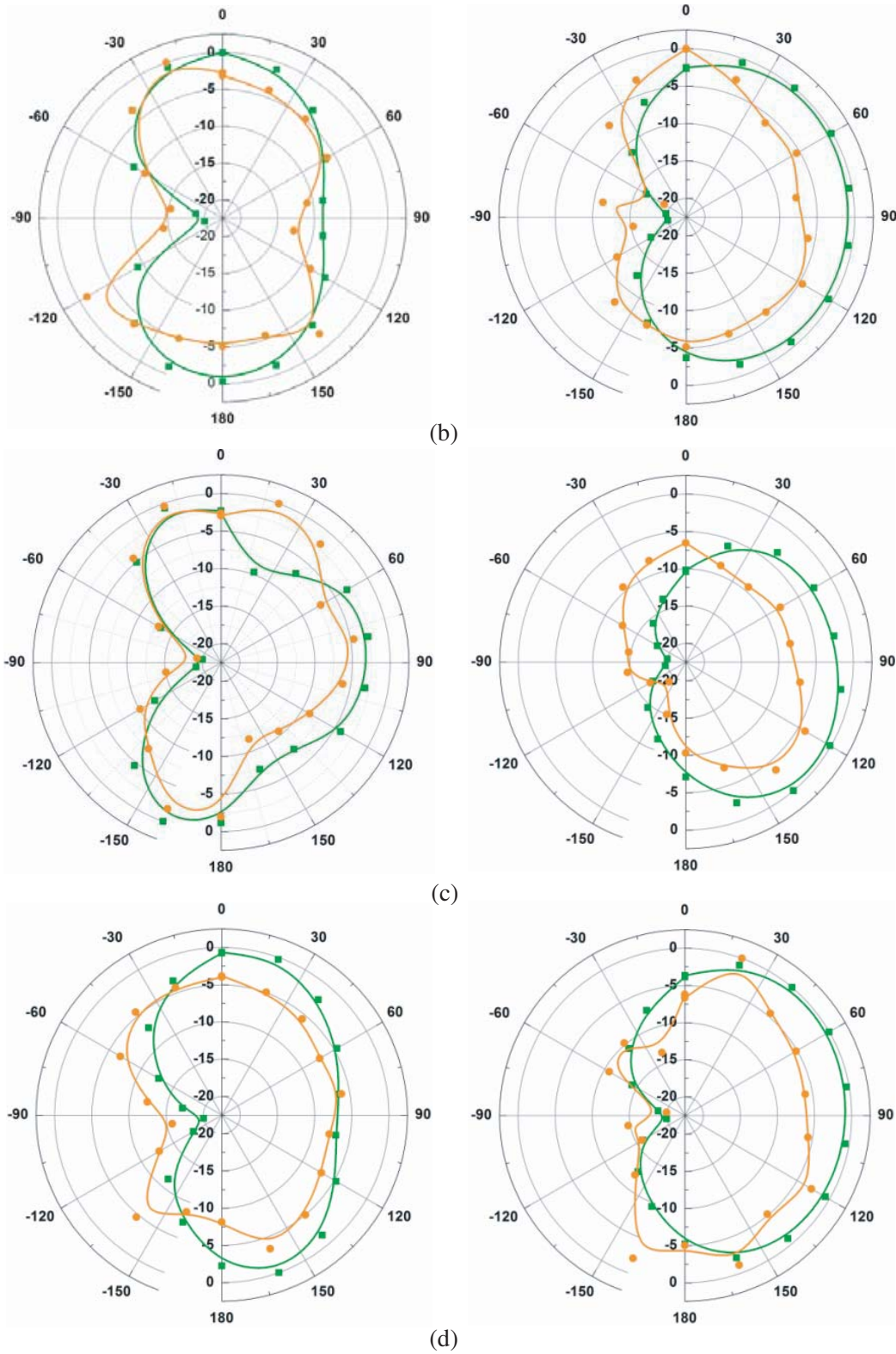
Figure 14. H plane (left) and E plane (right) pattern at frequencies (a) $f_1 = 1.35\,\text{GHz}$, (b) $f_2 = 2\,\text{GHz}$, (c) $f_3 = 3.8\,\text{GHz}$ and (d) $f_4 = 5.22\,\text{GHz}$.
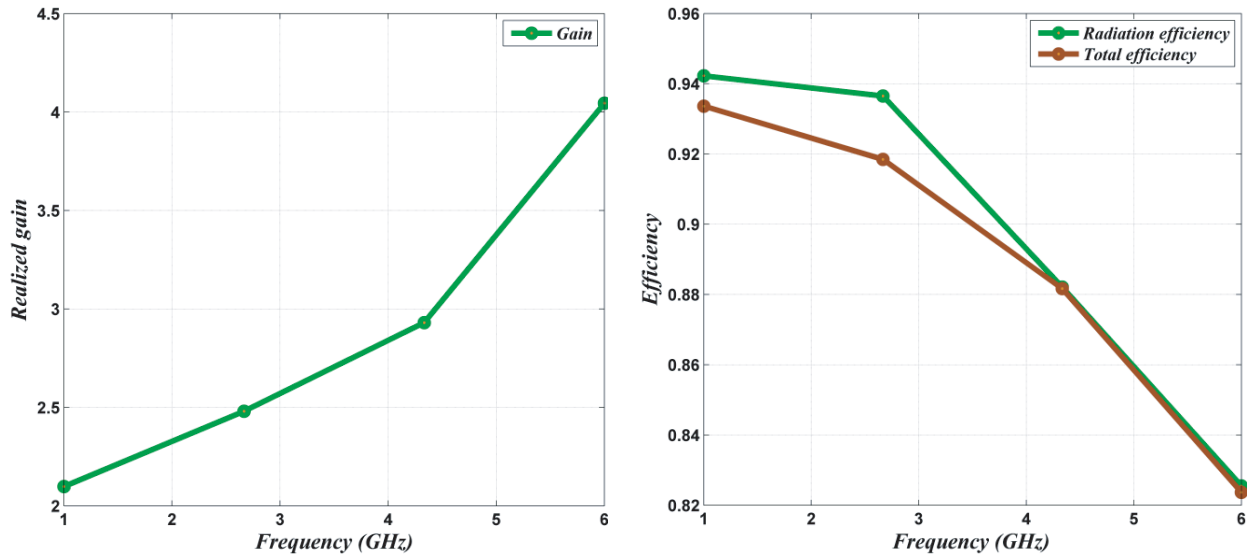
Figure 15. The simulated realized gain and efficiency of the proposed antenna.

Table 4. Comparison of proposed antenna with existing open slot antenna.

Reference	Dimensions (mm^2)	Bandwidth (%)	Substrate	Frequency range (GHz)
[7]	30 × 35	130.30	FR4	2.3–10.9
[10]	9.2 × 9.8	48	RT5880LZ	5–8.17
[17]	25 × 25	117.5	FR4	2.88–11.08
[19]	40 × 20	-	FR4	1.54–1.61 2.31–2.72 3.10–3.75 5.03–5.95
[18]	30 × 35	131	FR4	2.3–11.1
Proposed	66 × 45	121.14	FR4	1.375–5.6

investigated that the efficiency (Radiation and total efficiency) of the antenna is declined as operating frequency increases, which is because of dielectric loss. The comparison of proposed antenna with existing open slot antennas in terms of size and bandwidth is shown in Table 4. All these antennas are designed on an FR-4 and RT5880LZ substrate. The proposed antenna exhibits good impedance bandwidth. To cover lower frequency band, the size of proposed antenna is larger than other.

7. CONCLUSION

The stepped open slot antenna with a circular tuning element is simulated, fabricated, and tested with the help of Vector Network Analyzer N2223A in frequency range 1 to 6 GHz. After investigation, it is noticed that the step size of stair, radius of tuning stub, and major axis radius of elliptical slot critically affect the impedance matching and bandwidth of the antenna. The proposed antenna exhibits the measured fractional bandwidth of 121.14% for $S_{11} < -10$ dB which covers the frequency range from 1.375 to 5.6 GHz. This antenna also exhibits the resonance at frequencies (measured) 1.625, 2.52, 2.82, 3.75, 4.67, and 5.42 GHz. At the best matching frequencies 1.35, 2, 3.8, and 5.22 GHz, the current distribution is analyzed, and series of equation are deduced. The simulated and measured radiation patterns are compared in both planes. The omni-directionality is lost due to higher order modes, and asymmetry pattern is found due to the structure.

REFERENCES

1. Tang, M. C., R. W. Ziolkowski, and S. Xiao, "Compact hyper band printed slot antenna with stable radiation properties," *IEEE Transactions on Antennas and Propagation*, Vol. 62, No. 6, 2962–2969, June 2014.

2. Shinde P. N. and J. P. Shinde, "Design of compact pentagonal slot antenna with bandwidth enhancement for multiband wireless applications," *AEU — International Journal of Electronics and Communications*, Vol. 69, 1489–1494, 2015.

3. Jan, J. Y. and J. W. Su, "Bandwidth enhancement of a printed wide-slot antenna with a rotated slot," *IEEE Transactions on Antennas and Propagation*, Vol. 53, 2111–2114, 2005.

4. Jan, J. Y. and L. C. Wang, "Printed wideband rhombus slot antenna with a pair of parasitic strips for multiband applications," *IEEE Transactions on Antennas and Propagation*, Vol. 57, 1267–1270, 2009.

5. Ellis, M. S., Z. Zhao, J. Wu, Z. Nie, and Q. H. Liu, "Small planar monopole ultra wideband antenna with reduced ground plane effect," *IET Microwave Antennas Propagation*, Vol. 9, 1028–1034, 2015.

6. Liu, J., S. Zhong, and K. P. Esselle, "A printed elliptical monopole antenna with modified feeding structure for bandwidth enhancement," *IEEE Transactions on Antennas and Propagation*, Vol. 59, 667–670, 2011.

7. Chen, W. S. and K. Y. Ku, "Bandwidth enhancement of open slot antenna for UWB applications," *Microwave and Optical Technology Letters*, Vol. 50, 438–439, 2008.

8. Wang, C. J., M. H. Shih, and L. T. Chen, "A wideband open-slot antenna with dual-band circular polarization," *IEEE Antennas and Wireless Propagation Letters*, Vol. 14, 1306–1309, 2015.

9. Wang, C. J. and W. B. Tsai, "Microstrip open-slot antenna with broadband circular polarization and impedance bandwidth," *IEEE Transactions on Antennas and Propagation*, Vol. 64, 4095–4098, 2016.

10. Al-Azza, A. A., F. J. Harackiewicz, and H. R. Gorla, "Very compact open-slot antenna for wireless communication systems," *Progress In Electromagnetics Research Letters*, Vol. 51, 73–78, 2015.

11. Deshmukh, A. A. and K. P. Ray, "Formulation of resonance frequencies for dual-band slotted rectangular microstrip antennas," *IEEE Antennas and Propagation Magazine*, Vol. 54, No. 4, 78–97, 2012.

12. Deshmukh, A. A. and G. Kumar, "Broadband compact V-slot loaded RMSAs," *Electronics Letters*, Vol. 42, 1, 2006.

13. Kamakshi, J. A. Ansari, A. Singh, and A. Mohammad, "Desktop shaped broadband microstrip patch antenna for wireless communication," *Progress In Electromagnetics Research Letters*, Vol. 50, 13–18, 2014.

14. Gopikrishna, M., D. D. Krishna, C. K. Aanandan, P. Mohanan, and K. Vasudevan, "Design of a microstip fed step slot antenna for UWB communication," *Microwave and Optical Technology Letters*, Vol. 51, 1126–1129, 2009.

15. Gopikrishna, M., D. D. Krishna, C. K. Aanandan, P. Mohanan, and K. Vasudevan, "Compact linear tapered slot antenna for UWB applications," *Electronics Letters*, Vol. 44, 1–2, 2008.

16. Zong, W. H., X. M. Yang, S. Li, X. Y. Qu, and X. Y. Wei, "A compact slot antenna configuration for ultrawideband (UWB) terminals and mobile phones," *Int. J. RF Microw. Comput. Aided Eng.*, Vol. 28, 1–8, 2018.

17. Song, K., Y. Z. Yin, B. Chen, and S. T. Fan, "Bandwidth enhancement design of compact UWB step-slot antenna with rotated patch," *Progress In Electromagnetics Research Letters*, Vol. 22, 39–45, 2011.

18. Song, K., Y. Z. Yin, X. B. Wu, and L. Zhang, "Bandwidth enhancement of open slot antenna with a T-shaped stub," *Microwave and Optical Technology Letters*, Vol. 52, 390–393, 2010.

19. Ren, W., S. W. Hu, and C. Jiang, "An ACS-fed F-shaped monopole antenna for GPS/WLAN/WiMAX applications," *International Journal of Microwave and Wireless Technologies*, Vol. 9, 1123–1129, 2017.

20. Chen, B., Y. C. Jiao, F. C. Ren, L. Zhang, and F. S. Zhang, "Design of open slot antenna for bandwidth enhancement with a rectangular stub," *Progress In Electromagnetics Research Letters*, Vol. 25, 109–115, 2011.

21. Singh, A., M. Aneesh, and J. A. Ansari, "Analysis of microstrip line fed patch antenna for wireless communications," *Open Engineering*, Vol. 7, 279–286, 2017.

22. Pawar, S. S., M. Shandilya, and V. Chaurasia, "Parametric evaluation of microstrip log periodic dipole array antenna using transmission line equivalent circuit," *Engineering Science and Technology, an International Journal*, Vol. 20, 1260–1274, 2017.

23. Singh, A., M. Aneesh, K. Kamakshi, and J. A. Ansari, "Circuit theory analysis of aperture coupled patch antenna for wireless communication," *Radioelectronics and Communications Systems*, Vol. 61, 168–179, 2018.